SANDIA REPORT

SAND2012-8025
Unlimited Release
Printed September 2012

Functionalized Ultra-Porous Titania Nanofiber Membranes as Nuclear Waste Separation and Sequestration Scaffolds for Nuclear Fuels Recycle

Haiqing Liu, Nelson Bell, Benjamin B. Cipiti, Tom G. Lewis, Dorina F. Sava, Tina M. Nenoff

Prepared by
Sandia National Laboratories
Albuquerque, New Mexico 87185 and Livermore, California 94550

Sandia National Laboratories is a multi-program laboratory managed and operated by Sandia Corporation, a wholly owned subsidiary of Lockheed Martin Corporation, for the U.S. Department of Energy's National Nuclear Security Administration under contract DE-AC04-94AL85000.

Issued by Sandia National Laboratories, operated for the United States Department of Energy by Sandia Corporation.

Available to DOE and DOE contractors from
U.S. Department of Energy
Office of Scientific and Technical Information
P.O. Box 62
Oak Ridge, TN 37831

Telephone: (865) 576-8401
Facsimile: (865) 576-5728
E-Mail: reports@adonis.osti.gov
Online ordering: http://www.osti.gov/bridge

Available to the public from
U.S. Department of Commerce
National Technical Information Service
5285 Port Royal Rd.
Springfield, VA 22161

Telephone: (800) 553-6847
Facsimile: (703) 605-6900
E-Mail: orders@ntis.fedworld.gov
Online order: http://www.ntis.gov/help/ordermethods.asp?loc=7-4-0#online

SAND2012-8025
Unlimited Release
Printed September 2012

Functionalized Ultra-Porous Titania Nanofiber Membranes as Nuclear Waste Separation and Sequestration Scaffolds for Nuclear Fuels Recycle

Haiqing Liu, Nelson Bell, Benjamin B. Cipiti, Tom G. Lewis, Dorina F. Sava, Tina M. Nenoff

Sandia National Laboratories
P.O. Box 5800
Albuquerque, NM 87185-1415

Abstract

Advanced nuclear fuel cycle concept is interested in reducing separations to a simplified, one-step process if possible. This will benefit from the development of a one-step universal getter and sequestration material so as a simplified, universal waste form was proposed in this project. We have developed a technique combining a modified sol-gel chemistry and electrospinning for producing ultra-porous ceramic nanofiber membranes with controllable diameters and porous structures as the separation/sequestration materials. These ceramic nanofiber materials have been determined to have high porosity, permeability, loading capacity, and stability in extreme conditions. These porous fiber membranes were functionalized with silver nanoparticles and nanocrystal metal organic frameworks (MOFs) to introduce specific sites to capture gas species that are released during spent nuclear fuel reprocessing. Encapsulation into a durable waste form of ceramic composition was also demonstrated.

Acknowledgement

This work was funded by the Separations Working Group as part of the Fuel Cycle Technologies program under the Department of Energy, Nuclear Energy. Sandia National Laboratories is a multi-program laboratory managed and operated by Sandia Corp., a wholly owned subsidiary of Lockheed Martin Corporation, for the U.S. Department of Energy's National Nuclear Security Administration under contract DE-AC04-94AL85000.

Table of Contents

Figures

Acronyms

MOC	Modified Open Cycles
AIROX	Atomics International Reduction-Oxidation
LWR	Light Water Reactor
SNF	Spent Nuclear Fuel
DUPIC	Direct use of spent PWR fuel in CANDU
MPACT	Nuclear material management campaign
MOF	Metal organic frameworks
$Ti(OiPr)_4$	Titanium isopropoxide
RH	Relative humidity
SEM	Scanning electron microscopy
HR-TEM	High-resolution transmission electron microscopy
STEM	Scanning transmission electron microscopy
HAADF	High-angle annular dark-field
SEAD	Selected area electron diffraction
EDX	Energy dispersive X-ray
XRD	Powder X-ray diffraction
ZIF	Zeolitic imidazolate framework
Hmim	2-methylimidazole
AcOH	Acetic acid
BET	Brunauer-Emmett-Teller

1.0 INTRODUCTION

This report assembles the methodology, characterization, and preliminary results of developing thermally stable ultra-porous polycrystalline ceramic nanofiber membranes as nuclear waste separation and sequestration scaffolds for nuclear fuels, in particular Modified Open Cycles (MOC). By combining a modified sol-gel chemistry and coaxial electrospinning, amorphous TiO_2 nanofibers were first obtained by electrospinning, and subsequently converted to anatase fibers with controllable interior porous structures via calcination without changing their morphology. We anticipate that by crushing the fuel and performing a simplified heating and/or hot gas extraction process, we will be able to separate out the volatile fission products (e.g. Cs, Sr, Rb) and poisons (e.g. Xe) by using such ceramic nanofiber membranes as specific absorbent materials, which subsequently can be disposed in encapsulated glass waste forms. Functionalized ceramic nanofiber membranes are being examined for gas separations for these various dry separations options, as an innovative one-step extraction process in modified open fuel cycle.

The sol-gel technique has been widely employed in the generation of many kinds of ceramic materials in the form of films, fibers, nanoparticles, and monoliths [1]. Ceramic fibers, in particular, have been shown to be very useful for applications in separation and catalysis as supports due to their extraordinary mechanical and chemical stability at extreme conditions. Some template-directed sol-gel processes have been developed to synthesize ceramic fibers and tubes by, for example, using anodic alumina membranes, patterned polymer grooves, or supermolecular self-assembled structures [2-4]. However these methods all generally involve multiple steps and the product yield is often quite limited.

The electrospinning technique is an electrostatically induced assembly process, and is an efficient, inexpensive, and scalable approach to synthesize nanofibers [5-7]. In a typical electrospinning process, a viscoelastic polymer solution is ejected from a metallic nozzle under a strong external electric field. Electrostatic charges are therefore built up on the surface of the polymer solution. When the repulsive force between these charges overcomes the surface tension of the fluid, an electrified liquid jet is induced, which is uniaxially and extensively stretched to form continuous thin fibers and gets deposited on the collection screen. The morphology and diameter of the electrospun fibers depends upon material properties, including molecular weight, viscosity, electrical conductivity, and surface tension of the solvent, as well as operational conditions, including strength of the electric field, feeding rate, separation distance between source and collector, and humidity.

There are two unique morphological characteristics of porous nanofiber membranes: porous open structures that provide low resistance to mass transport, and large volumetric surface area that provide high efficiency of target-absorbent fiber membrane interaction. One can also extend this method to process many different types of ceramic nanofibers by simply changing the sol-gel precursors, including the technologically important metal oxides TiO_2, SiO_2, Al_2O_3, V_2O_5, ZrO_2, $MgTiO_3$, CeO_2, SnO_2, $BaTiO_3$, or mixed oxides. Enhanced affinity and selectivity to the radionuclide contaminants of interest can be achieved by functionalizing the porous surface of the nanofiber membranes with both chemisorption and physisorption, and

porous nanofibers can serve as excellent support for other extremely high surface area nanomaterials (MOFs, zeolites, etc).

In the present study, we demonstrate a successful method of producing porous titania nanofibers through a modified sol-gel technique in conjunction with coaxial electrospinning. Polycrystalline nanofibers made of anatase TiO_2 were chosen to demonstrate the concept, and subsequent functionalization was added onto the fiber membranes to study the iodine separations and glass encapsulation in final waste forms. In particular, we first functionalized the nanofibers with silver (Ag) nanoparticles for iodine sorption studies as proof of concept for gas capture at lower temperatures; then we functionalized the nanofibers with MOFs for both iodine capture and for extension to high temperature MOC off gases, such as Xe capture. This invention could have a direct impact on the spent fuel separations as it could significantly reduce the cost and complexity of reprocessing, provide a much simpler plant with a small footprint and small number of waste streams. It will also be an important element of an integrated energy and waste management policy.

Advanced modeling and simulation based on neutronic characterization of spent nuclear fuel (SNF) in a simplified modified open cycle that undergoes Atomics International Reduction-Oxidation (AIROX) or enhanced oxidation/ chlorination process, is being investigated in parallel with this project. The goal of the modeling work is to determine the effect on neutronics and heat load of recycling the leftover products back into light water reactors (LWR). Further details are reported by Lewis, et al, 2012, in FCRD-SWF-2012-000259[8].

2.0 BACKGROUND

The principal reason for reprocessing used nuclear fuel is to recover and extract unused fissile materials in order to provide fresh fuel for existing and future nuclear power plants. Reprocessing can save up to 30% of the natural uranium otherwise required. A second reason is to reduce the volume of high-level waste to be disposed. Although fuel reprocessing by itself does not reduce radioactivity or heat generation and therefore does not eliminate the need for a geological waste repository, limited fuel recycling can provide an advantage of delaying the need for a repository for several decades.

The goal of a modified open fuel cycle is to develop a simpler reprocessing concept that reduces the cost of reprocessing while performing limited recycling. The recovered fuel would be blended with fresh uranium oxide and refabricated into fuel for recycling back into LWR. There are two key constraints on fuel recycling: the heat load and the negative reactivity effect of the fission products and actinides generated in the process. These poisons absorb neutrons and need to be offset with a more significant U-235 enrichment that is usually not desirable.

We propose a simplified process for re-using used LWR fuel that involves stripping the cladding, crushing the fuel to be able to remove select components, and then re-fabricating into fuel with the addition of fresh fuel. This combined *fuel/waste management idea* pulls from the DUPIC cycle (but is flexible enough in design to also be used in any recycle process that involves voloxidation, such as the dry chlorination process currently under development). We anticipate that by crushing the fuel and performing a simplified heating process and/or hot gas extraction process, we will be able to separate out the volatile fission products (eg., Cs, Sr, Rb) and poisons (eg., Xe) and allow recycle of the fuel through mixing with fresh fuel and re-sintering.

Because solvent extraction based aqueous reprocessing can be very complex and expensive due to the large number of tanks, large volume of solvents, safeguards, and security regulations, we are interested in utilizing membrane technology in high temperature dry processing using oxidation or a combination of oxidation and dry chlorination to remove volatile fission gases and poisons [9-10]. Such a processing step can be used at the head end of aqueous processing [11], to remove radionuclides that are major contributors to nuclear waste toxicity, so that the cost of aqueous-based used-fuel treatment can be reduced.

In particular, there are several advantageous reasons to explore high-porosity ceramic nanofibrous membrane materials for nuclear fuel reprocessing:

(1) Membrane morphology allows easy insertion in off-gas streams and removal afterwards, which is one main advantage comparing to most nanomaterials composed of dispersed particles.

(2) High-porosity membranes are high surface area high flux structures; therefore accessibility to large available surface area assures high loading capacity.

(3) Electrospun ceramic fibers membranes have good chemical, mechanical, and radioactive durability, and are also flexible compositional matrices such that incorporation of separations

materials and captured gases are suitable for low temperature encapsulant waste form. Such a one-step processing will require no purification or further separations.

(4) Electrospun fibers are an industrially scalable technology.

The overall goal of this work was to explore an innovative one-step extraction process that can separate out the volatile fission products and poisons by using functionalized ultra-porous ceramic nanofiber membranes as absorbent materials, to reduce the cost of aqueous-based used fuel treatment; consequently, to develop highly durable and leach-resistant waste forms of ceramic composition for safe, long-term waste disposal.

3.0 EXPERIMENTAL

3.1 Sol-gel precursor preparation

In a typical procedure, two solutions were prepared separately. One is a polymer solution of polystyrene (PS) dissolved in a DMF/THF solution. The second is the sol-gel precursor, titanium isopropoxide ($Ti(OiPr)_4$), with a binding polymer, polyvinylpyrrolidone (PVP), in anhydrous ethanol. Titanium isopropoxide is stabilized and complexed with different molar ratios of glacial acetic acid to control the hydrolysis and condensation reactions.

3.2 TiO_2 Nanofiber fabrication

The fabrication method is based on a modified electrospinning method of two solutions (Figure 1). The solutions are delivered through nozzles with the flow rates controlled by syringe pumps. The sol-gel precursor hydrolyzes and condenses to generate an inorganic gel network as the mixture is electrospun into the air. In the meantime, as the solvents evaporate quickly in the spinning process, two polymer phases separate to generate nanoscale domains within the metal oxide gel. In the after-process calcination step at elevated temperature, the sol precursor is converted into the desired ceramic, and both polymer components are removed. The exact method is covered under a Technical Advance submitted to Sandia National Laboratories for filing as a US Patent, in SD# 12197[12].

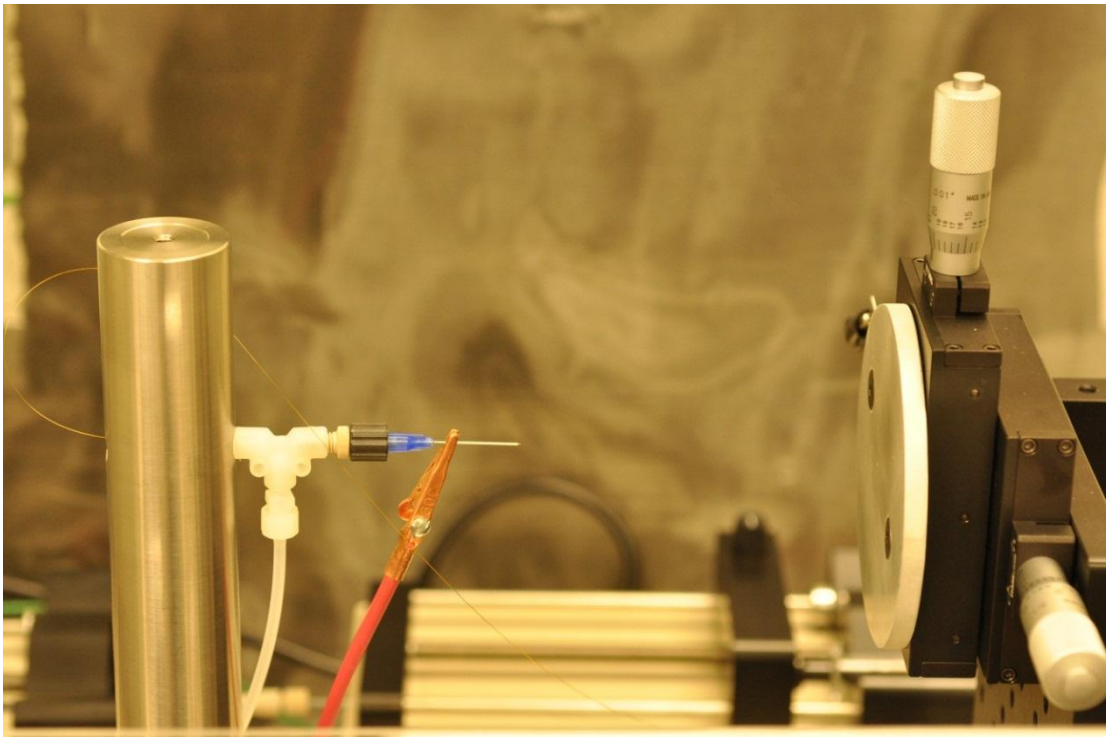

Figure 1: Photograph of electrospinning setup for fabricating porous titania nanofibers.

3.3 Annealing

After electrospinning, $Ti(OiPr)_4$ was allowed to hydrolyze at room temperature for 1 hour. Optimal conditions for calcination were established to completely burn off the PVP and PS, while retaining nanofiber morphology composed of crystalline TiO_2. For annealing temperatures below 450°C, complete pyrolysis of polymer does not occur; for annealing temperature above 650°C, mixed phases of TiO_2 appear. Based on extensive experiments, an optimal anneal temperature of 500°C was established. The as-spun compound nanofibers were peeled off the aluminum foil and transferred to a ceramic boat for annealing in a furnace at 500°C for 1 hour, to completely convert from amorphous $Ti(OiPr)_4$ to polycrystalline TiO_2, as well as to remove PS and PVP components. The annealed fiber membranes were allowed to cool slowly to room temperature afterwards.

3.4 Characterization

The morphology of the obtained titania nanofibers was characterized by means of electron microscopy. The nanofiber membrane was dispersed in ethanol in an ultrasonic bath and deposited by dipping onto carbon-coated copper grids. Scanning electron microscopy (SEM) characterization was performed on a FEI Nova NanoSEM operated at 5 kV, with a TLD lens, equipped with an energy-dispersive X-ray (EDX) spectrometer for compositional analysis. High-resolution transmission electron microscopy (HR-TEM) characterization was performed on a FEI Tecnai F30 TEM operated at 300 kV for bright field imaging, for dark-field imaging with a scanning TEM (STEM) system, and for selected area electron diffraction (SEAD) pattern analysis.

X-ray diffraction (XRD) analysis was performed using a SIEMENS D5000 powder X-ray diffractometer. Rotating detector scan was done over a range of 2θ angles from 5° to 85°, and step size of 0.05°.

3.5 Gas sorption measurements

Gas adsorption isotherms of the TiO_2 fiber membranes were measured at 77K, using a Micromeritics ASAP 2020 surface area and porosity analyzer. Nitrogen of ultra-high purity 99.999% (Matheson Tri-Gas) was used in these experiments. The fiber membranes are very light due to the material low density, therefore ethanol was used to wet the membrane and help to transfer into the long-neck glass tube for BET experiment. The samples were then completely dried in 90^{o}C, and degassed before BET.

3.6 Functionalization with Ag coating, iodine capture, and waste form fabrication

3.6.1 UV photoreduction of Ag particles on TiO_2 nanofibers

TiO_2 nanofiber membranes were immersed in 0.05 M $AgNO_3$ in H_2O/methanol (60/40 v/v) for 30 minutes in a quartz vial. The samples were then exposed to UV (302 nm) at 1.5 mW/cm^2 for 1 ~ 10 minutes to reduce $AgNO_3$ to Ag nanoparticles grafted on the TiO_2 electrospun nanofibers. The samples were rinsed in ethanol and dried in air at room temperature. The setup is shown in Figure 2.

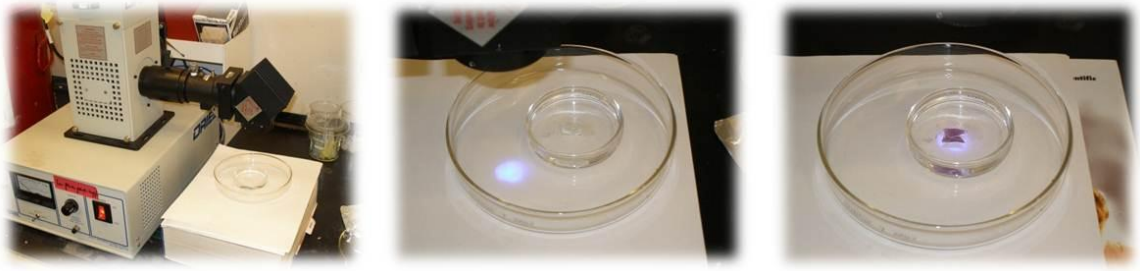

Figure 2. Photoreduction of $AgNO_3$ by UV radiation bonds Ag metal particles to the TiO_2 electrospun nanofibers.

3.6.2 Chemical reduction of Ag nanoparticle on TiO_2 nanofibers

TiO_2 nanofiber membranes were soaked in 1 mM $AgNO_3$ in H_2O solution for 1 hour. The sample was brought to boiling while stirring. 1% sodium citrate solution was gradually added to the boiling sample and stirring continued, which caused the fiber membrane to change color from white to black. The samples were rinsed in ethanol and dried in air at room temperature.

3.6.3 Iodine capture by Ag/TiO_2 fiber membranes

Iodine (I_2) permeation experiment was performed on Ag coated TiO_2 fibers by citrate reduction method. The Ag/TiO_2 fiber membranes were exposed to I_2 vapor at 90^{o}C in air for 15 hours, followed by 12 hour degas to remove excess I_2 and to yield fully loaded Ag/TiO_2. The morphology of AgI on TiO_2 fiber membrane was examined by SEM, and the presence of the elements Ag and I was confirmed by EDAX. The samples were analyzed by powder X-ray diffraction and examined by HR-TEM also.

3.6.4 Waste form

Simulated iodine waste form samples were made by mixing the low sintering temperature Bi-Si-Zn-Oxide glass powder (EG2922, Ferro Corp, Cleveland, OH) [13-15] with AgI/TiO_2 fibers. The fiber membrane was placed in between glass powder layers on a silicon wafer. The samples were then heated to 550^{o}C in air for 1 hour to sinter the glass.

3.7 Functionalization with nanocystal MOFs

Nanocrystal Zealitic imidazolate framework (ZIF)-8 based on chemistry of $Zn(NO_3)_2$ and 2-methylimidazole (Hmim) in methanol was made based on reference [18]. The presence of the ZIF-8 was confirmed by SEM.

The ZIF-8 nanoparticles were redispersed in fresh methanol by ultrasonic agitation. 10 wt% of ZIF-8 nanoparticles were added to the metal oxide precursor phase and mixed by vortex. The composite material was loaded into the syringe for electrospinning to make MOF functionalized composite TiO_2 nanofibers, as shown in Figure 3.

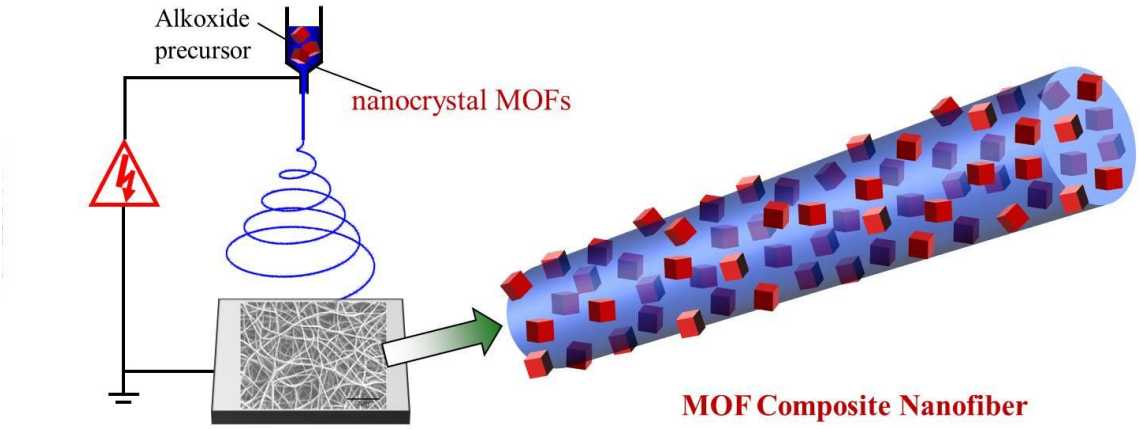

Figure 3. Schematics of incorporating MOFs into porous titania nanofibers to make nanocomposite fibers.

4.0 RESULTS AND DISCUSSION

Polycrystalline nanofibers made of anatase TiO_2 were chosen for proof of concept studies. Anatase phase was obtained through a modified sol–gel route from titanium isopropoxide modified with acetic acid in order to control hydrolysis and condensation reactions [19]. The use of acetic acid as modifier allows the control of both the degree of condensation and oligomerization of the precursor and leads to the preferential crystallization of TiO2 in the anatase phase.

4.1 Screen for most optimal experimental conditions

The degree of porosity of the nanofibers were found be to mostly impacted by catalyst to metal oxide precursor ratio and humidity in our experiments. A matrix study of fabricating porous titania nanofibers were completed, which included a total eight combinations of conditions of the catalyst to precursor ratio and the humidity. Figure 4 shows two sets of experiments conducted under relative humidity (RH) of 60% and 30%, and each RH set was done with different ratios of catalyst modifier acetic acid (AcOH) to titania precursor (Ti), 1:1, 2:1, 3.3:1, 5:1, respectively. It was found that humidity plays a strong role under these conditions: 60 % RH leads to bead formation, whereas 30% RH produces more uniform width. [AcOH]/[Ti] ratios in the middle range are superior for fiber size. The best and most stable parameters of fabricating nanofibers with highest degree of porosity were identified to be at 30% RH and [AcOH]/[Ti]=2. Figure 5 shows the high-resolution SEM examination of the TiO_2 nanofibers fabricated under these conditions, presenting variations in fiber porosity, thickness, and roughness morphology.

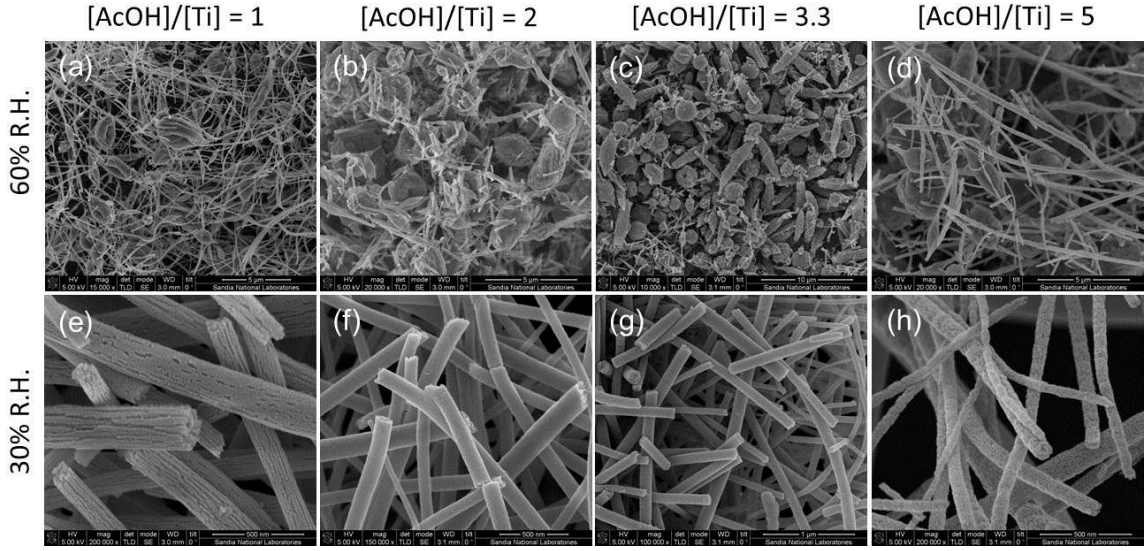

Figure 4. SEM images of titania nanofibers produced under different conditions of RH and [AcOH]/[Ti]. (a)-(d) were at 60% RH, and (e)-(h) at 30% RH.

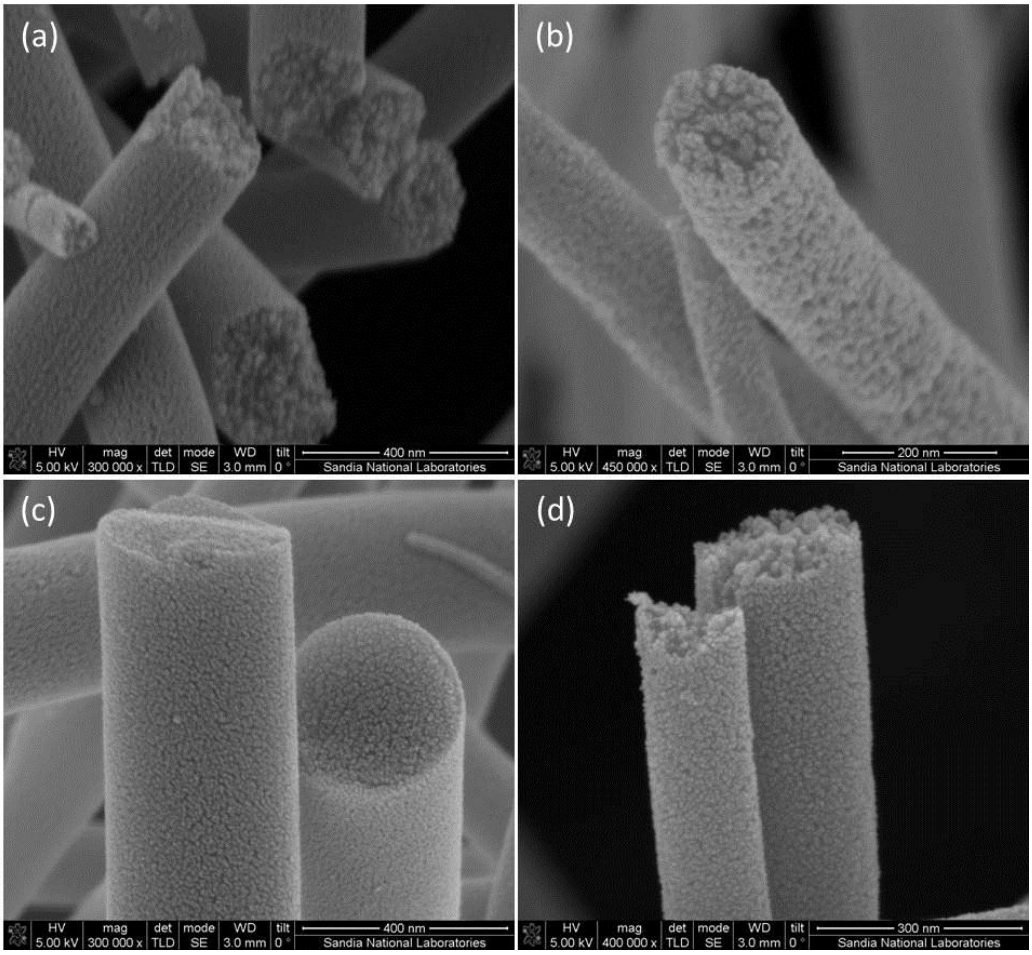

Figure 5. SEM examination of the TiO_2 nanofibers fabricated under conditions of RH = 30%, [AcOH]/[Ti] = (a) 1:1, (b) 2:1, (c) 3.3:1, (d) 5:1. Variations in fiber porosity, thickness, and roughness morphology were observed.

The most optimal condition at 30% RH, and [AcOH]/[Ti]=2 was used to produce large quantity of nanofiber membranes. The final product of the titania fiber membranes after calcination is shown in Figure 6. The ceramic membrane is a freestanding whole piece that is not fragile and is easy to transport.

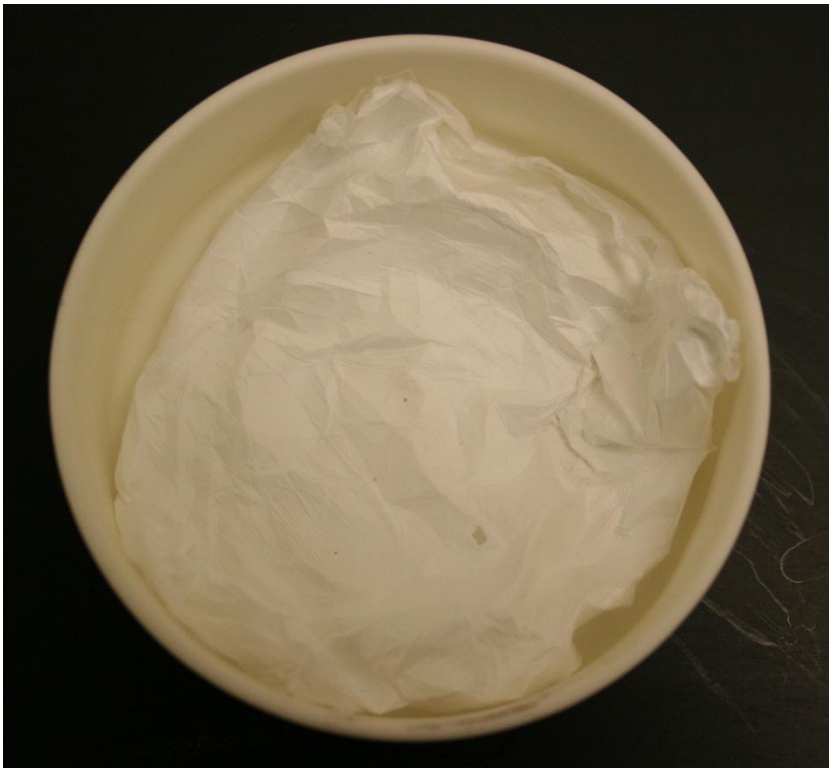

Figure 6. A bright field optical image of the titania fiber membranes. The diameter of the membrane is ~ 10 cm.

4.2 Microstructural characterization of TiO_2 nanofibers

SEM results suggest the integrative fiber membrane morphology prepared under 30% RH and [AcOH]/[Ti]=2 (Figure 7(a) and (b)), and the porous fiber structure and dimension (Figure 7(c) and (d)). The fibers diameters are mostly in the range of 50-200 nm, and the fibers are highly porous with fine pore sizes in the range of 2-10 nm. The non-woven TiO_2 nanofiber membranes provide two types of porous structures: the relatively large pores (primary pores) formed through the interconnection of nanofibers, and pores with much smaller sizes (secondary pores) within individual nanofibers.

EDX analysis was done to confirm the elemental information of TiO_2 nanofiber membranes. In Figure 8, the EDX spectrum obtained from a representative area of the sample showed the presence of Ti and O peaks, suggests the final fiber product is composed of TiO_2 only.

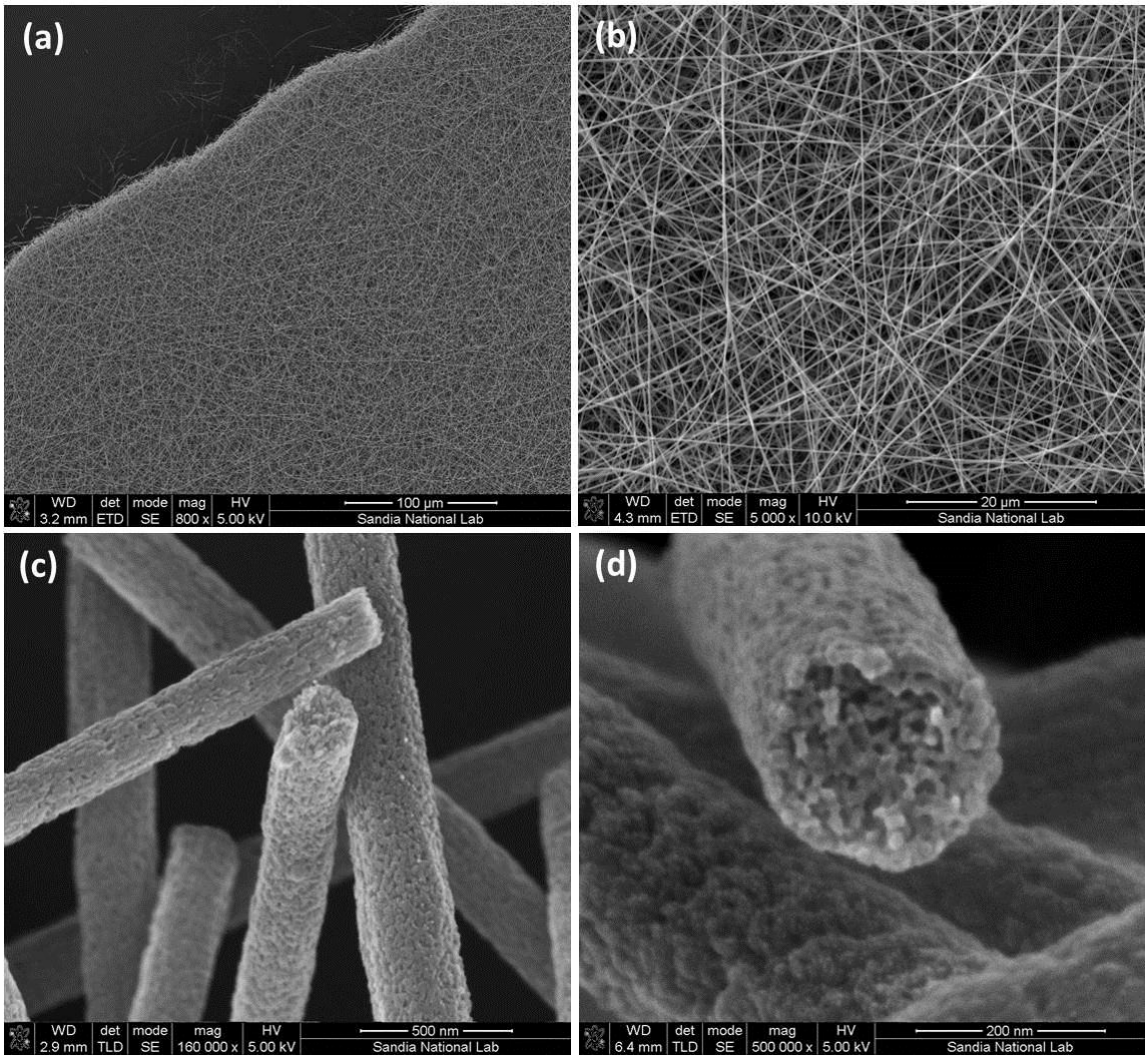

Figure 7. Progressively higher magnification of the scanning electron microscopy (SEM) image of the titania nanofibers. (a) and (b) show the membrane morphology; close-up images (c)and (d) show the porous structures of the nanofibers.

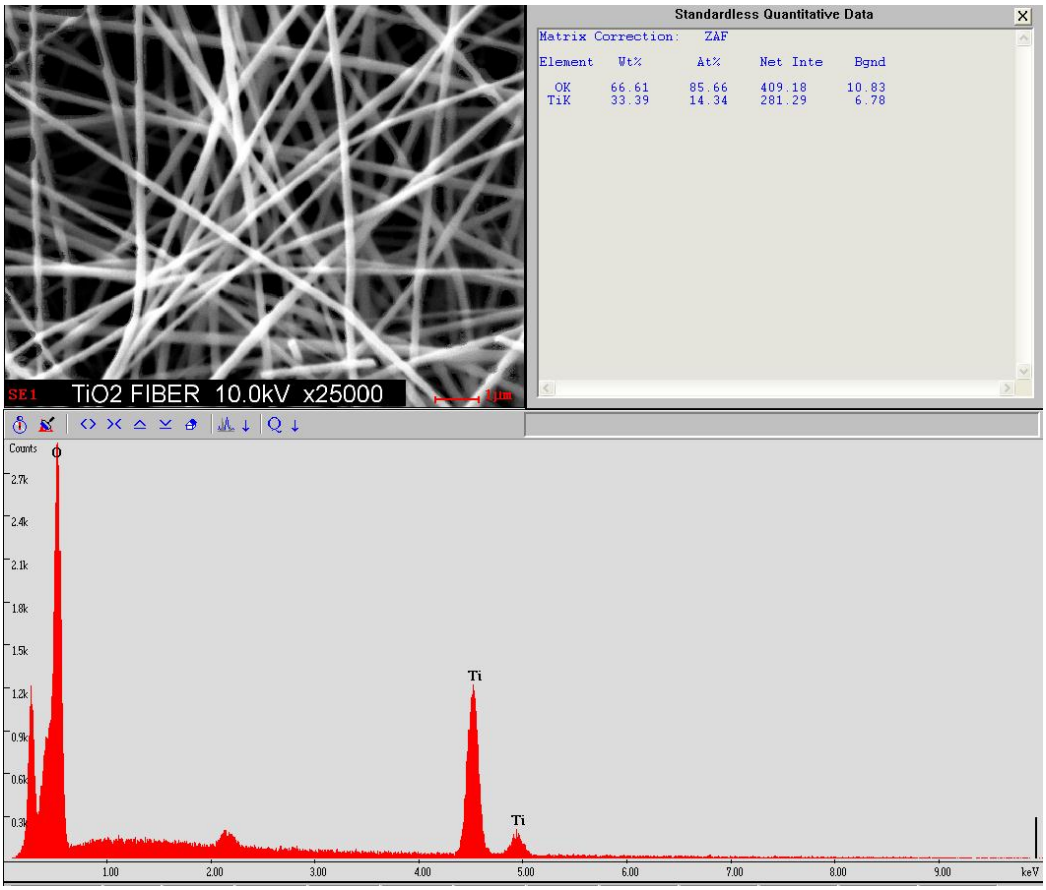

Figure 8. EDX spectrum from a representative area of TiO_2 nanofibers showing presence of Ti and O peaks.

The crystalline structure including the phase purity was examined by powder XRD. The calcined nanofibers were found to be completely crystalline. Figure 9 indicates the fibers have the polycrystalline anatase structure, as all diffraction peaks can be indexed to those of the anatase phase of titania. It is known that anatase phase is superior to rutile phase of TiO_2 for gas sensitivity, catalytic, and photochemical applications [16].

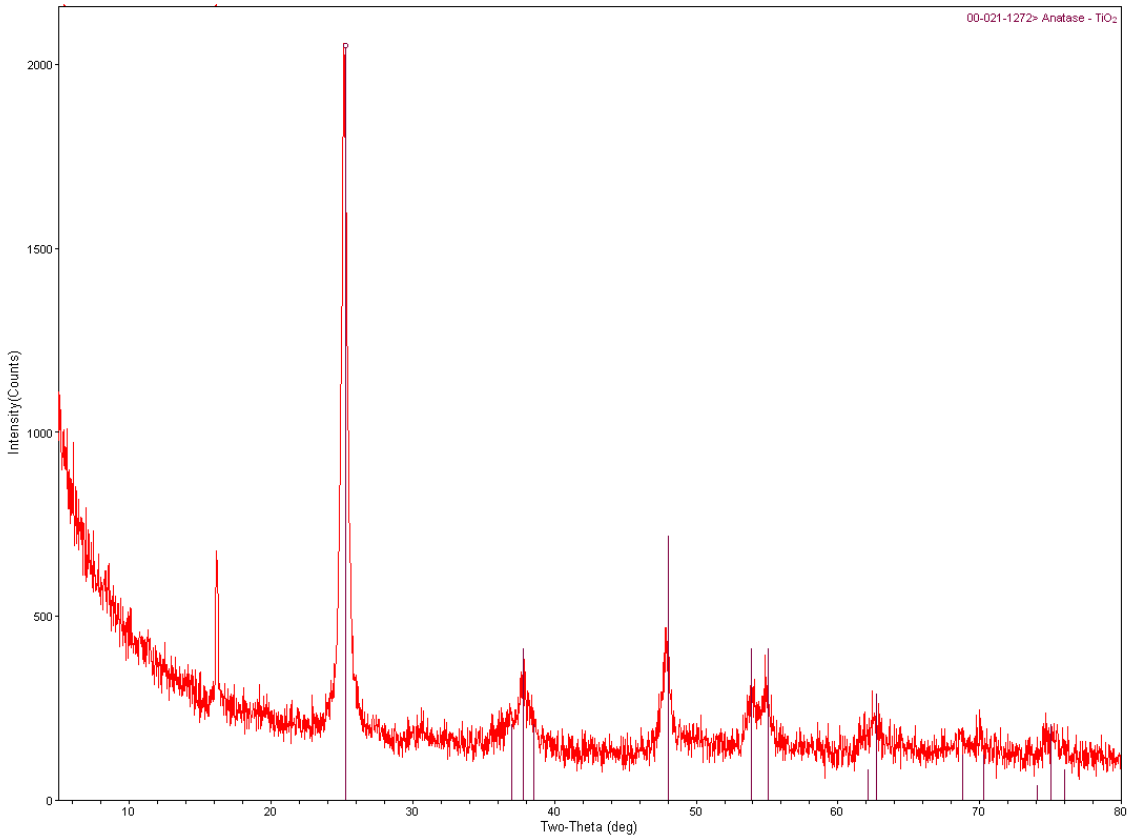

Figure 9. Powdered X-ray Diffraction analysis of porous titania nanofibers after calcinations suggests it to be anatase phase.

The microstructural morphology of the TiO_2 nanofibers was characterized by means of HR-TEM. Figure 10(a) (b) shows bright-field TEM image taken from a single anatase TiO_2 nanofiber, confirmed the crystalline sizes from few to tens of nanometers. Figure 10 (c) shows the electron diffraction pattern of a selected area in the nanofiber, revealing the polycrystalline nature. Figure 10(d) is a HR-TEM image provides detailed information on the nanostructure of the TiO_2 nanofiber. The lattice fringe spacing of about 0.351 nm is assigned to d-spacing of {101} crystal planes, which is characteristic to the anatase phase. These electron diffraction results are in good agreement with the previous XRD results suggesting the polycrystalline anatase phase of these nanofibers.

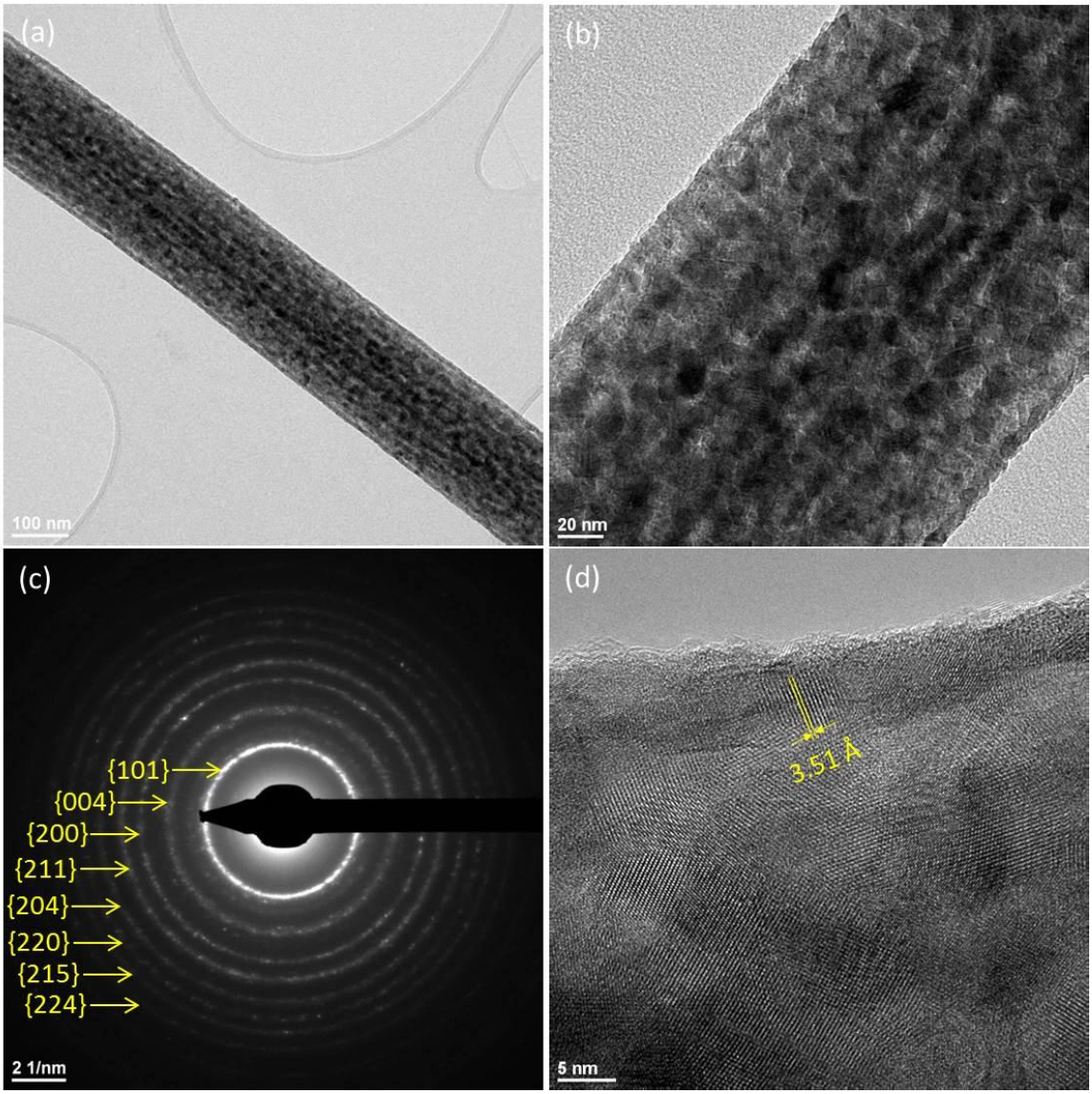

Figure 10. (a)(b) Bright-field TEM image of anatase TiO_2 nanofibers suggest the porous structures. (c) Selected area electron diffraction pattern showing polycrystalline nature of anatase, with all the peaks matching anatase phase. (d) HR-TEM image showing grains of anatase oriented in {101} direction, with lattice fringes of 0.351 nm corresponding to anatase {101} planes.

4.3 Surface area analysis

Nitrogen adsorption–desorption isotherms from Brunauer-Emmett-Teller (BET) surface area analysis measurements are shown in Figure 11. The curves suggest a type IV-like isotherm for mesoporous materials [17]. The adsorption started straight indicating a single layer of nitrogen adsorption on the material surfaces, followed by the capillary condensation of nitrogen as the relative pressure (P/P_0) increased past 0.8, which can be due to the nitrogen condensed within the porous structures of nanofibers. BET surface area analysis indicates the specific surface area of titania nanofiber membrane is 57.1 m^2/g, and the Langmuir Surface Area is 79.3

m^2/g. Four runs of analysis on the same sample were conducted and no obvious hysteresis was observed. The pore size distribution is based on DFT N_2 Tarazona NLDFT model (inset of Figure 11), and majority pores are in the range of 20 nm.

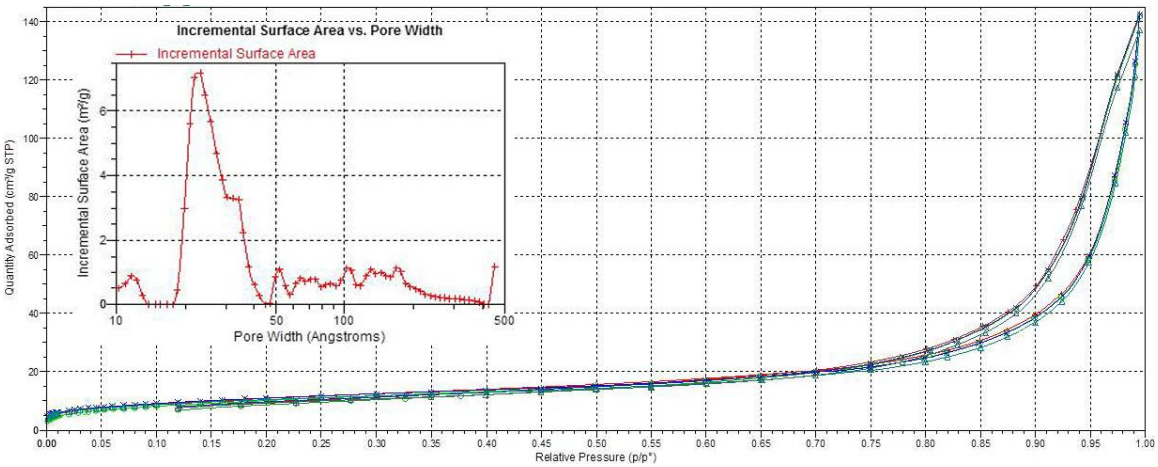

Figure 11. BET surface area analysis. The isotherm data fit to Type IV Isotherm. There were 4 runs of analysis on the same sample as indicated with different colored curves. The inset shows the pore size distribution that was determined, indicating that the majority of pores are about 20 nm.

X-ray diffraction pattern (Figure 12) suggests that the anatase TiO_2 phase maintained before and after the BET test. The samples were wet in ethanol when loading for BET experiment, which may contribute to get the anatase structure more crystalline. This may explain the relatively higher peak observed in after BET test.

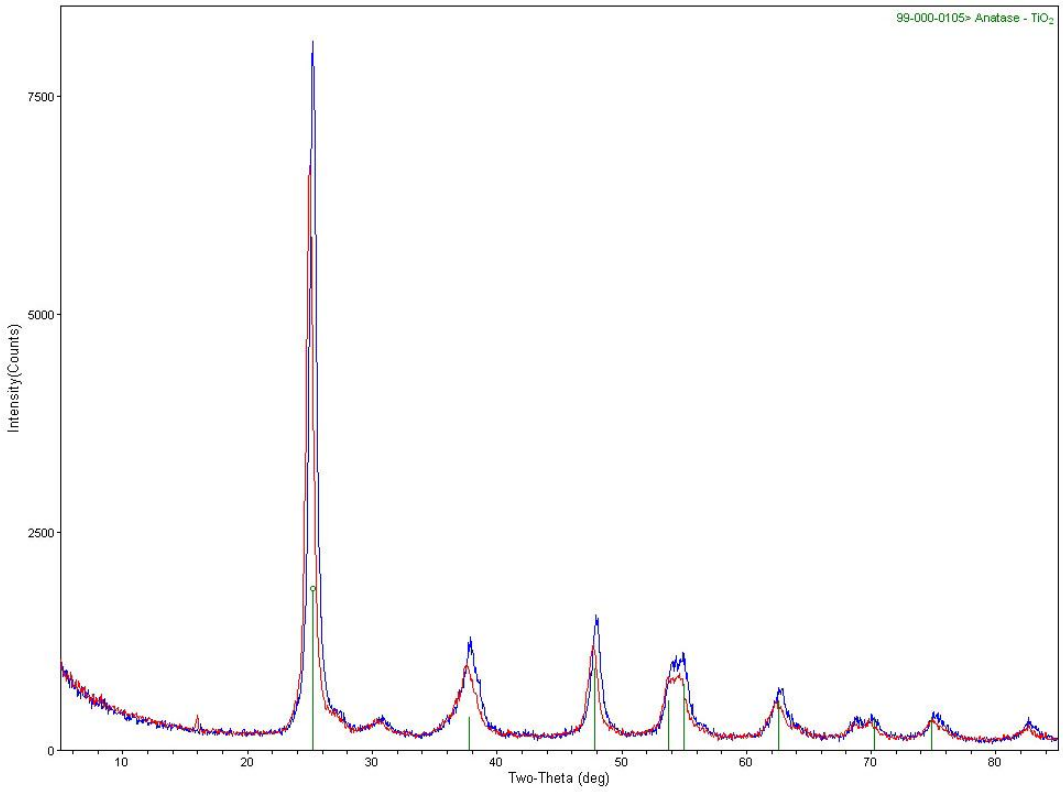

Figure 12. X-ray diffraction pattern suggest the anatase TiO_2 phase maintained before (red) and after (blue) the BET test.

4.4 Ag-TiO_2 nanofiber membranes, I_2 capture, and waste form formation

Sorption onto silver-containing zeolite mordenite is a benchmark for radiological iodine capture. In this proposal, we investigated iodine capture based on porous TiO_2 nanofiber membranes that are functionalized with Ag nanoparticles. Though Ag-TiO2 might be of interest for next generation iodine capture materials, they are good test materials for functionalization work on the nanofibers.

The first approach to graft Ag nanoparticles onto TiO_2 nanofibers was by UV photoreduction. The TiO_2 nanofibers were soaked in $AgNO_3$ solutions first, then exposed to UV at 1~10 minutes time span. Possibly due to the very fast nucleation stage in this method, the Ag particles were effectively loaded onto TiO_2 nanofibers, which was confirmed by SEM (Figure 13(a) and (b)). However the size of the Ag particle was difficult to controll and the Ag particles are generally very large on the micron scale. The EDX spectrum (Figure 13(c)) obtained from a representative area of the sample showed the presence of Ti, O, and Ag peaks, suggests the Ag existing with the TiO_2 in the samples.

The second approach to coat Ag nanoparticles onto TiO_2 nanofibers was by citrate reduction. From SEM characterization (Figure 14(a)-(c)), the Ag nanoparticles were distributed

much more uniform and the particle sizes were also smaller (on tens of nanometer). EDX spectrum (Figure 14(d)) confirmed the presence of Ag with TiO_2. The citrate reduction approach was identified as a more optimal method to deposit Ag nanoparticles onto TiO_2 nanofibers, and was used for following I_2 capture experiment.

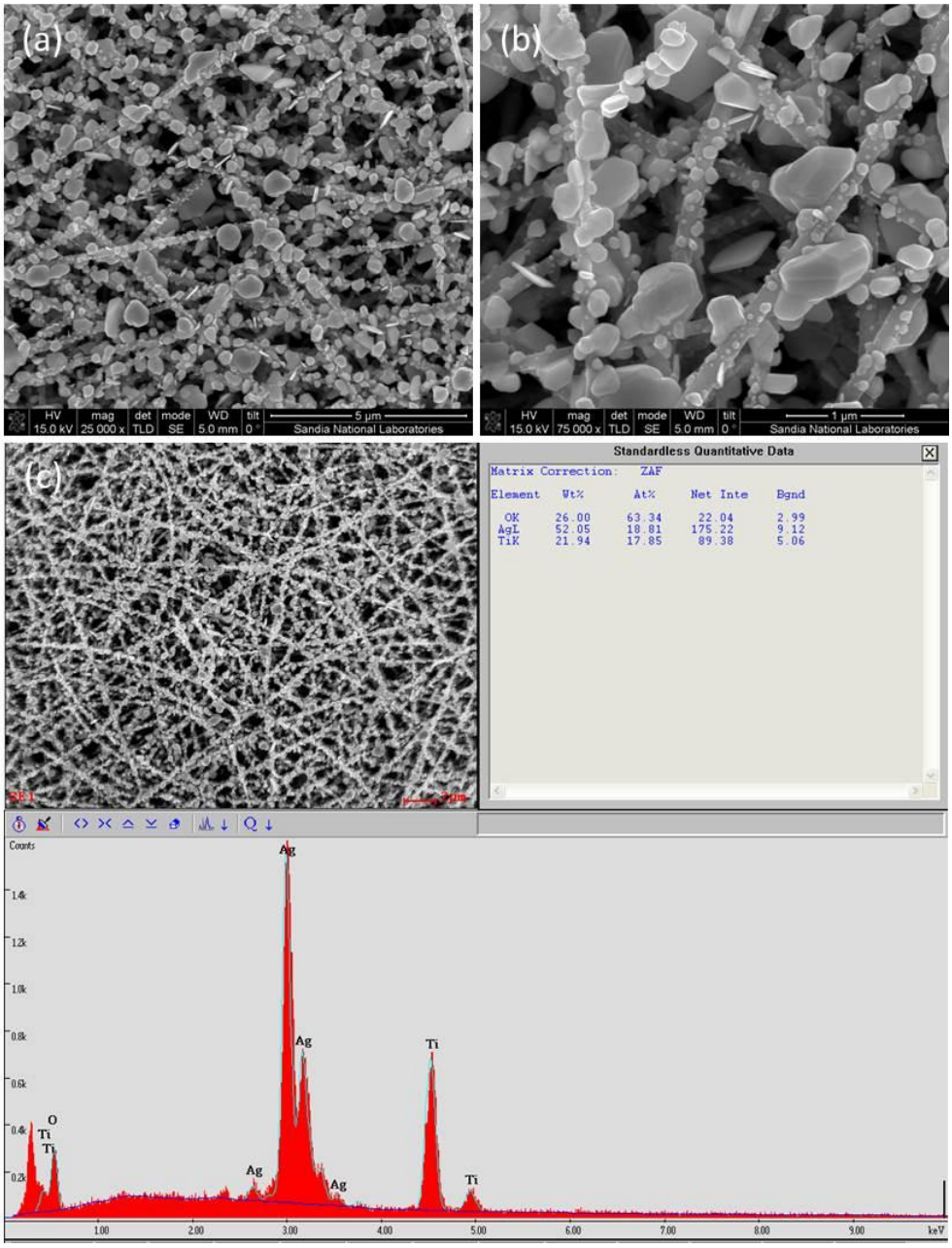

Figure 13. (a) (b) SEM of Ag deposited on TiO_2 fibers by UV photoreduction method. (c) EDX spectrum indicating the presence of Ti, O, and Ag peaks.

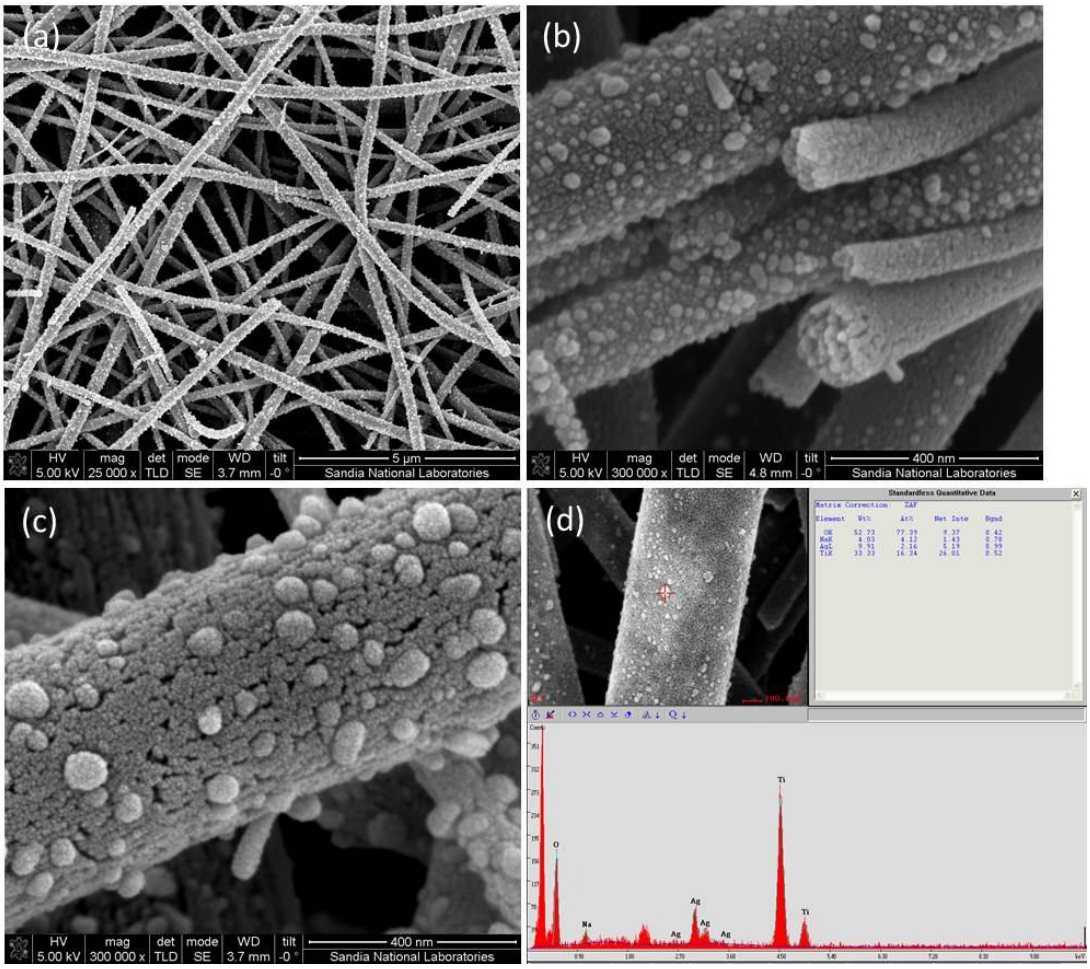

Figure 14. (a)-(c) SEM of Ag deposited on TiO_2 fibers by citrate reduction methhod. (d) EDX spectrum indicating the presence of Ti, O, and Ag peaks.

Bright-field TEM images (Figure 15(a)-(c)) were taken for the Ag on TiO_2 nanofiber samples. The small particles seen on the nanofibers are confirmed to be silver. Figure 15(c) is high-resolution TEM showing the evidence of Ag presence on anatase. The d-spacing measurements of the particle of 0.236 nm show close match to the Ag {111} crystal plane, and d-spacing measurements of the randomly oriented nanograins of 0.351 nm show close match to the anatase TiO_2 {101} crystal plane. The presense of silver crystal planes {111} is indicative of elemental Ag present in the nanofibers. TEM-EDX analysis was done to confirm the presence of Ag nanoparticles (data not shown). Scanning TEM and high-angle annular dark-field (STEM-HAADF) imaging was used to identify the distribution of Ag nanoparticles in the nanofibers. Figure 15(d) shows a STEM-HAADF image of a representative area of the sample. The large atomic number (Z) elements appear brighter than the lower Z elements, therefore the bright white spots are identified to be Ag nanoparticles due to its higher Z that distributed along the TiO_2 nanofiber everywhere. This confirms the presence of Ag nanoparticles rather than film type of coating of Ag on TiO_2 fibers.

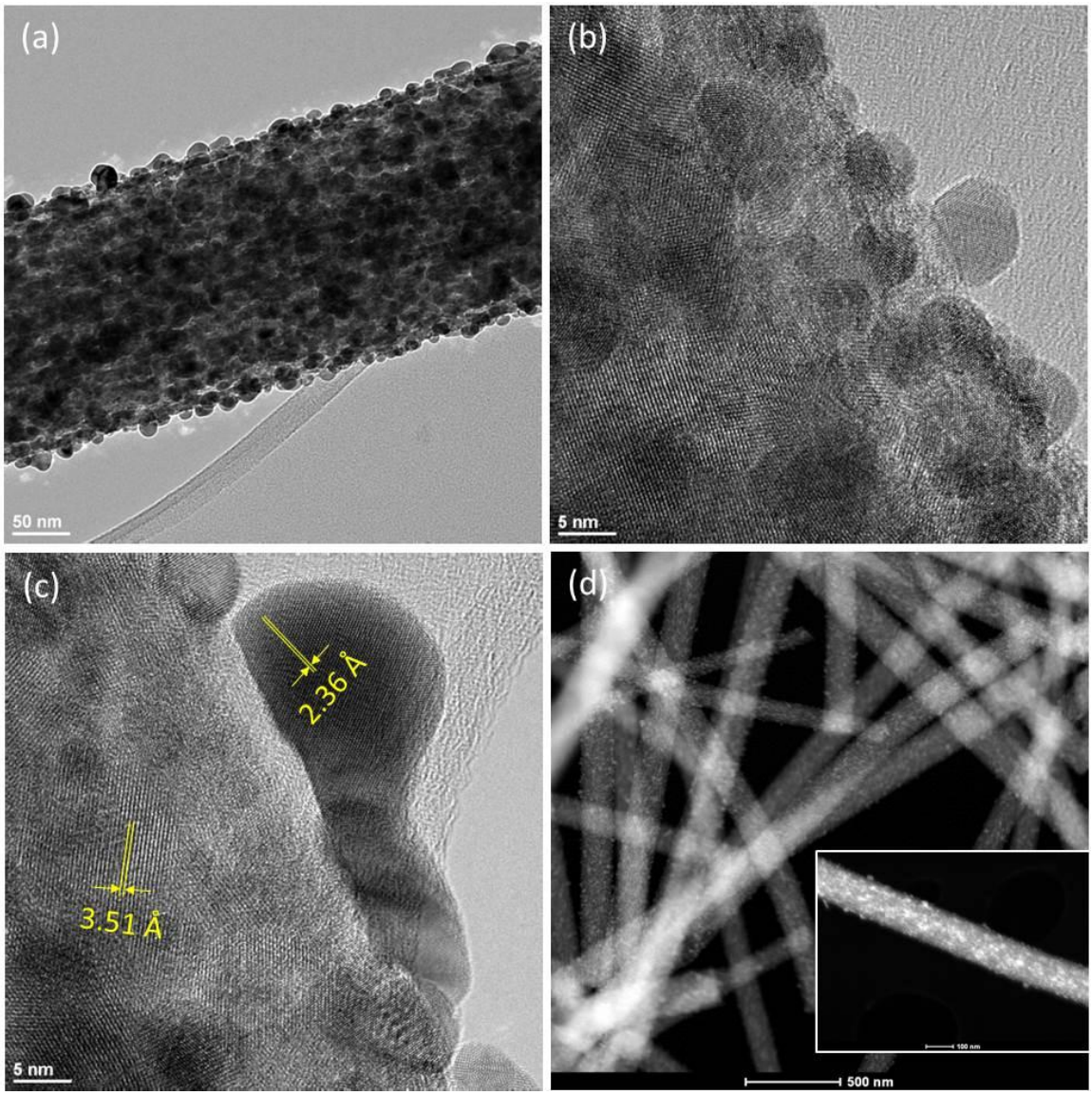

Figure 15. (a) Bright-field TEM image of Ag/TiO_2 nanofibers. (b)-(c) High-resolution TEM images of selected area showing the randomly oriented grains of anatase, as well as crystalline Ag nanoparticles. Lattice fringes corresponding to Ag {111} and anatase {101} planes are shown. (d) STEM-HAADF image of a representative area. Bright white spots represent the higher atomic number element Ag along the TiO_2 nanofibers, which are less bright area. The inset is a high-magnification HAADF image of the sample.

In the iodine permeation experiment, the fiber membranes turned whitish yellow color after absorbing I_2, indicating silver iodide (AgI) was formed. An EDX mapping (Figure 16) suggests that the presence of TiO_2 and AgI. There was some sodium contamination in the sample as seen in the mapping due to the sodium citrate used in the reduction experiment, and this contamination can be reduced in the future. However, even with a very low voltage of electron beam used, the AgI decomposed very fast, as revealed in Figure 17, the time study under SEM. Same problem existed when examining the AgI-TiO_2 samples under TEM.

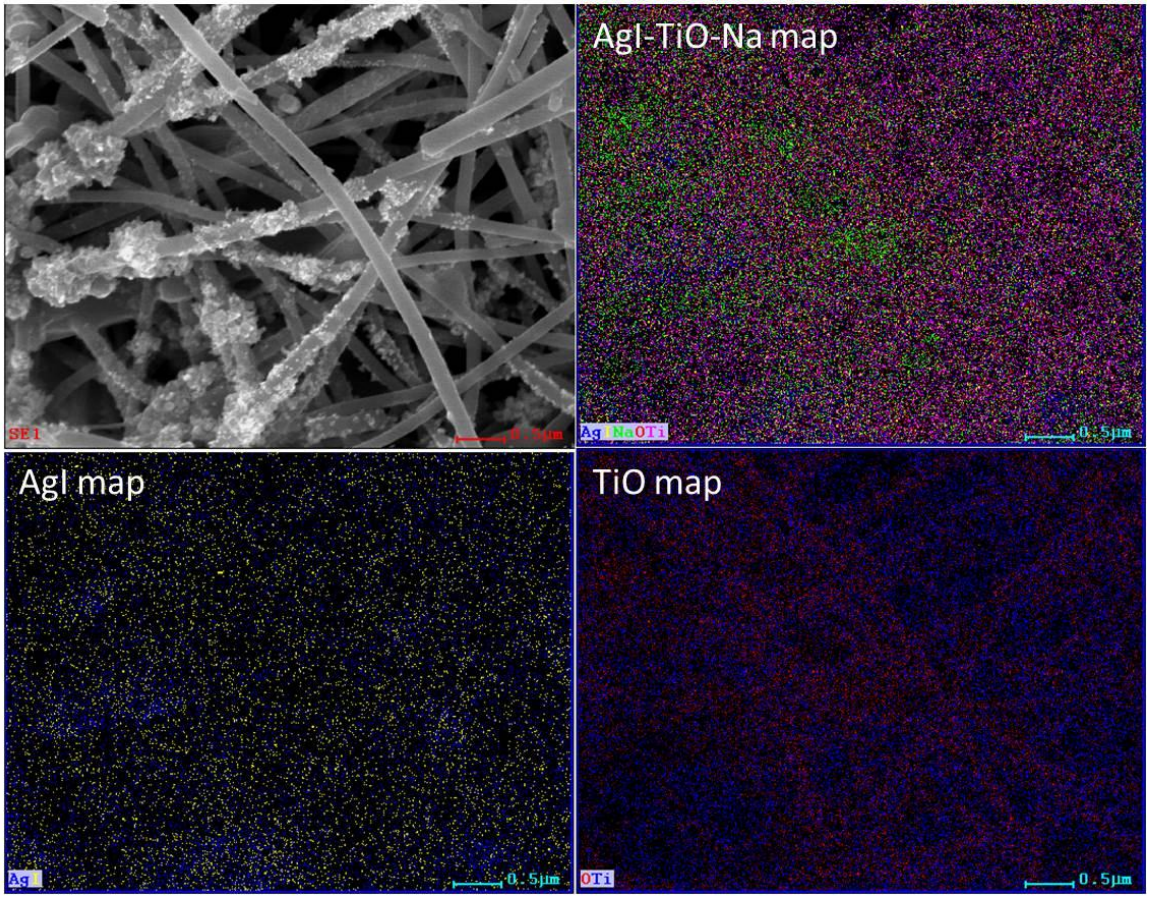

Figure 16. EDX mapping suggesting the presence of TiO_2 and AgI.

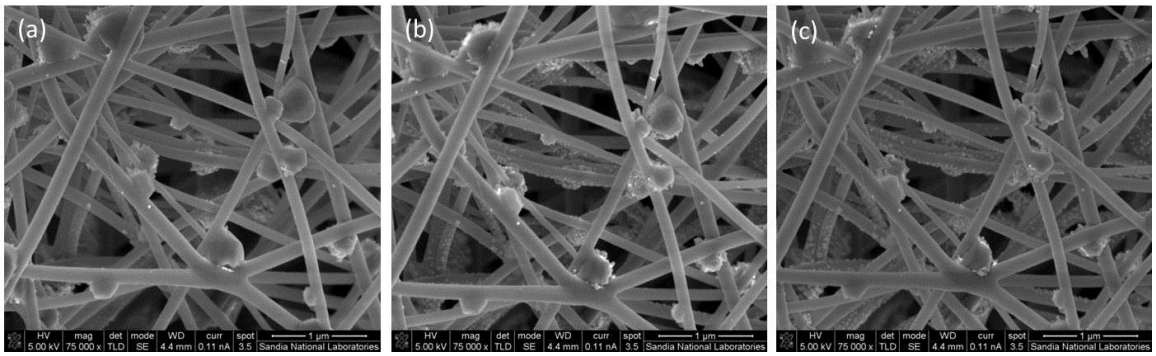

Figure 17. SEM of AgI on TiO_2 fibers membrane samples. The electron beam dwelling leads to AgI decomposing to Ag quickly. (a), (b), and (c) were images taken at 0.5, 2, and 5 minutes after electron beam dwelling.

A comparison study of selected area electron diffraction on TiO_2, Ag-TiO_2, and AgI-TiO_2 samples were conducted. Figure 18(a) reveals the polycrystalline structure of the anatase TiO_2 with all identifiable crystalline planes labeled. Figure 18(b) reveals an additional Ag {111} crystalline plane other than the anatase crystalline planes (labels omitted for clarifying look).

Figure 18(c) shows no obvious AgI crystalline planes rather than Ag and anatase crystalline planes, which suggests the AgI might have been gone on the onset of electron beam.

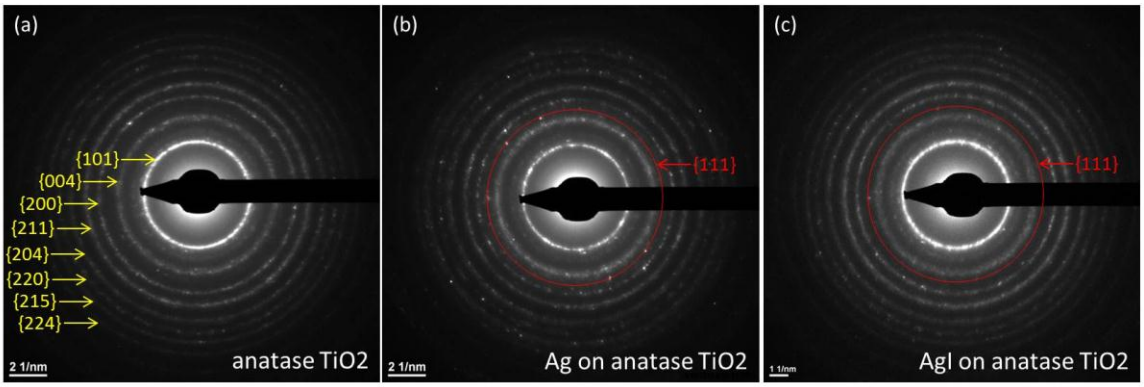

Figure 18. Comparison study of selected area electron diffraction on TiO_2, Ag-TiO_2, and AgI-TiO_2 samples. (a) anatase TiO_2, with all anatase crystalline planes; (b) Ag on anatase TiO_2, with Ag {111} crystalline plane; (c) AgI on anatase TiO_2, only Ag {111} crystalline plane identified, but no AgI phase.

Powder X-ray diffraction pattern showed anatase TiO2, as well as both cubic (Iodargyrite) and hexagonal (Miersite) phases of AgI, as identified in Figure 19. The γ-AgI formation is favored for I_2 vapor capture by metallic Ag [20]. γ-AgI structure forms by insertion of iodine into tetrahedral interstices in the fcc Ag° lattice, and may be diffusion limited.

In order to rationally optimize the I_2 capture process, it is important to understand the molecular basis for its performance, the properties of the silver iodide (AgI) formed on the nanopore supports, and the distribution of the AgI product. This requires a technique that can provide information on the local structure at the nanoscale, and probe the properties of individual component in this gas-solid reaction system. Due to the volatile nature of AgI, electron beam prevents one to get reliable SEM and TEM imaging and characterization of these systems. Highly penetrating high-energy X-ray measurement is therefore an ideal approach to minimize beam damage, and the X-ray scattering data can be used for PDF analysis to unveil the critical information for understanding this novel materials system. We plan to send samples to the Advanced Photon Source at Argonne National Laboratory to collect scattering data using the high-energy X-ray beamline, and for PDF analysis.

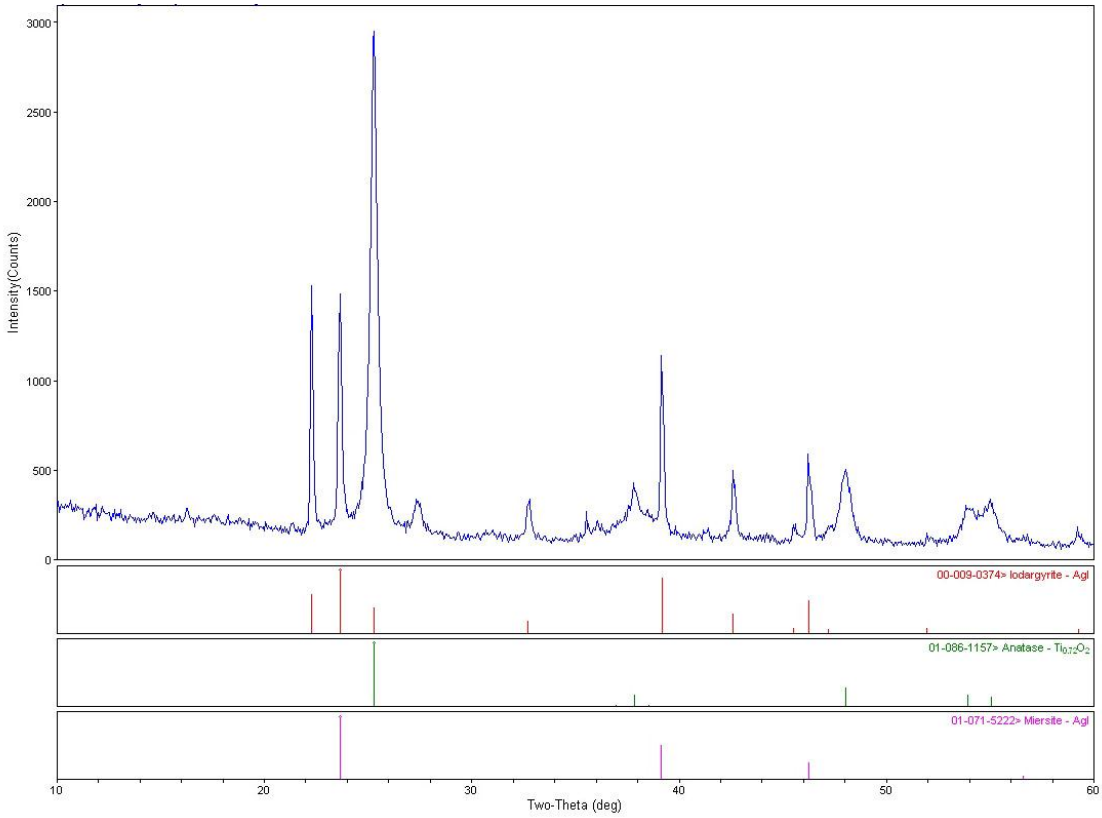

Figure 19. Powder X-ray diffraction pattern of AgI-TiO_2 sample suggesting the co-existence of cubic (Iodargyrite) and hexagonal (Miersite) phases of AgI, and the anatase.

AgI loaded TiO_2 fiber membrane was successfully encapsulated in glass waste form, as indicated in SEM examination shown in Figure 20. Wetting of the nanofibers is visible from the isolated melted glass material, as well as fiber immersion in molten glass. Mixtures of the glass waste form with AgI-TiO_2 were durable in aqueous environment. No cracking was found. Because the nanofibers can be synthesized from a large variety of metal oxides, we believe that their composition can be optimized both to incorporate the fission products released from the used fuel and for encapsulation into a durable inorganic waste form.

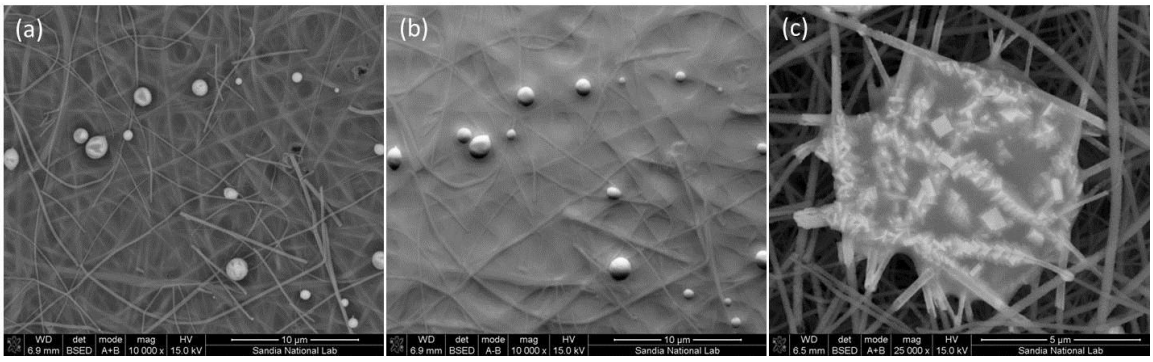

Figure 20. SEM of AgI loaded TiO2 fiber membranes encapsulated in glass waste form.

4.5 MOF-TiO_2 composite nanofibers

Research in our group has recently shown that molecular iodine gas can be successfully captured in large quantities in MOFs, such as the pore size restricted, and hydrophobic ZIF-8 framework [21-23]. As such, we believed that the successful incorporation of ZIF-8 into the nanofiber membranes would result in highly selective and high surface area composite membranes. Furthermore, gas sorption studies can confirm their applicability to fission gas capture abilities.

Nanocrystal ZIF-8 was successfully synthesized, with particle size about 80 nm and 35 nm, respectively (Figure 21), as confirmed by SEM.

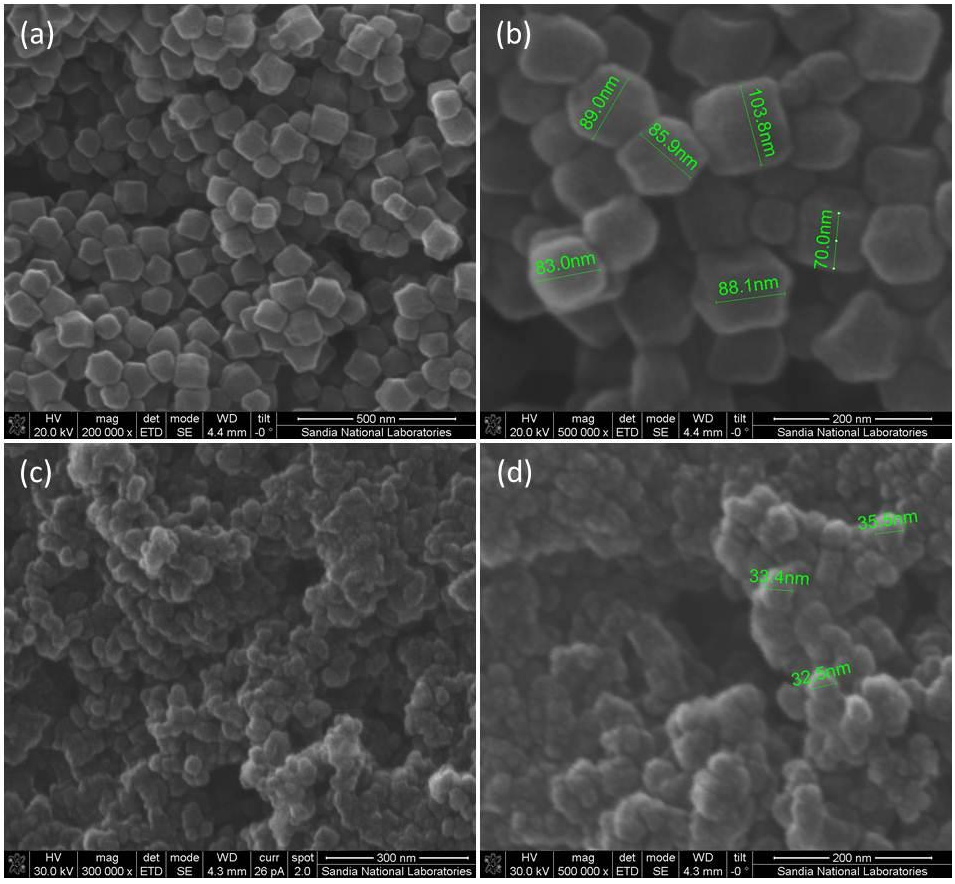

Figure 21. Synthesis of nanocrystal ZIF-8. (a) and (b) are nano ZIF-8 with particle size about 80 nm; (c) and (d) are nano ZIF-8 with particle size about 35 nm.

In order to create hierarchical nanofibers with high surface areas and good accessibility, the nano ZIF-8 were integrated into TiO_2 nanofibers to make a composite membrane. The MOF-TiO_2 composite nanofiber membranes were successfully made (Figure 22). Nitrogen adsorption test will be conducted to evaluate the accessibility of the composite fiber membranes.

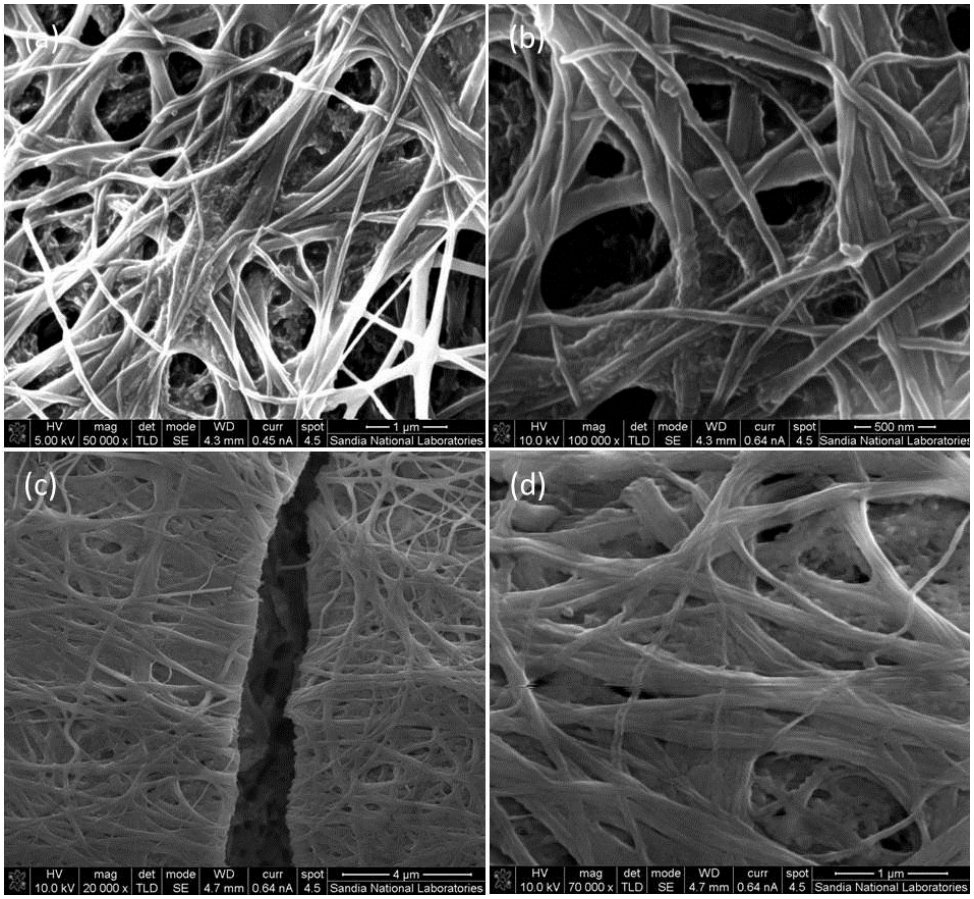

Figure 22. SEM of MOF-TiO_2 composite fiber membranes. (a)(b) before, and (c)(d) after calcination.

Our on-going research goals included the use of these materials (ZIF-8/TiO_2 membranes) in iodine gas sorption studies, to better understand if there is added sorption capacity of the composite membranes due to higher surface area, and if the iodine is better captured due to the size restriction of the ZIF-8 pores. Next steps in year 3 of this project included incorporation of Xe selective MOFs (synthesized and tested recently at PNNL) [24-25] into the nanofiber membranes for gas testing studies targeted at poison gas capture from the MOC fuel recycle processes. However, due to program redirection, the project is ending in FY12.

5.0 CONCLUSION

We have developed a technique for producing high-porosity ceramic nanofiber membranes with controllable diameters and porous structures, and demonstrated the functionalization of the membranes to capture gas species of interest in spent nuclear fuels. Such electrospun ceramic absorbent materials will have direct applications as nuclear and industrial waste cleanup and storage materials, and can be safely disposed of after encapsulated in glass waste form without the risk of leakage. The key advantage of this concept is to eliminate dissolution and reduce separations into a one-step process, which, in turn, will provide a much simpler plant with a small footprint and small number of waste streams. The one-step gettering and sequestration of the released gases and fission products provides a simplified and universal waste form, while allowing for a vast majority of the fuel to be recycled back into the fuel cycle.

This work currently has ties in an existing process (DUPIC) and an on-going research program in the separations campaign (dry chlorination), as well as the nuclear material management campaign (MPACT). Other alternative advanced fuel cycle research concepts have similar goals to reduce separations to a simplified, one-step process if possible. These concepts can all benefit from the development of a universal getter and sequestration material as proposed here. Expertise in the fuels campaign can be used to determine how the recycled fuels can be re-formed and what level of new fuel addition will be required. The use of stable, selective inorganic membranes will directly impact used fuel separations and systems work by significantly reducing the cost complexity of reprocessing, and contribute to secure and economic implementation of advanced fuel cycles in the United States.

6.0 REFERENCES

1. C.J. Brinker, "Sol-Gel Science: The Physics and Chemistry of Sol-Gel Processing", Academic Press, (1990)
2. B.B. Lakshmi, et al, "Sol−Gel Template Synthesis of Semiconductor Nanostructures", *Chem. Mater.* **9**(3): 857 (1997)
3. M. Bognitzki, et al., "Polymer, Metal, and Hybrid Nano- and Mesotubes by Coating Degradable Polymer Template Fibers", *Adv. Mater. 12(9): 637* (2000)
4. D.K. Yi, et al., "Spin-on-Based Fabrication of Titania Nanowires Using a Sol−Gel Process", *Nano Lett.* **2**(10): 1101 (2002)
5. Z.M. Huang, et al., "A review on polymer nanofibers by electrospinning and their applications in nanocomposites", *Composites Science and Technology*, **63**(15): 2223 (2003)
6. D. Li and Y. Xia, "Electrospinning of Nanofibers: Reinventing the Wheel?", *Adv. Mater.* **16**(14): 1151 (2004)
7. R.W. Tuttle, et al., Electrospun ceramic fibers: "Composition, structure and the fate of precursors", *Appl. Surf. Sci.* **254**: 4925 (2008)
8. T.G. Lewis, et al., "Modified Open Cycle Modeling". FCRD-SWF-2012-000259, July 2012; and SAND2012-5456, July 2012.
9. G.D. Del Cul et al, "Advanced Head-End Processing of Spent Fuel", 2005 ANS Annual Meeting; DOE/NE-SWG meeting, Albuquerque, NM (December 2010)
10. K.H. Kang, et al., "Fabrication of Simulated DUPIC Fuel", *Metals Mater.* **6**(6): 583 (2000)
11. "Engineering Alternatives Study", Savannah River Site (July 2007)
12. T.M. Nenoff, et al., "Nanoporous Ceramic Nanofiber Membranes for Highly Selective Gas/Ion Capture", Sandia Technical Advance, SD# 12197, Dec 2011.
13. Nenoff, et al., GNEP-WAST-PMO-MI-DV-2008-000149 (2008)
14. T.J. Garino, et al., "Low-Temperature Sintering Bi–Si–Zn-Oxide Glasses for Use in Either Glass Composite Materials or Core/Shell 129I Waste Forms", *JACerS*, **94**: 2412 (2011)
15. T.J. Garino, et al., "Development of Waste forms for Radioactive Iodine", *Ceramic Transactions*, 224 (2010)
16. X. Chen, et al., "Titanium Dioxide Nanomaterials: Synthesis, Properties, Modifications, and Applications", *Chem. Rev.* **107** (7):2891 (2007)
17. D. Grosso, et al., "Two-dimensional hexagonal mesoporous silica thin films prepared from block copolymers: detailed characterization and formation mechanism", *Chem. Mater.* **13**(5): 1848 (2001)
18. J. Cravillon, et al., "Controlling Zeolitic Imidazolate Framework Nano- and Microcrystal Formation: Insight into Crystal Growth by Time-Resolved In Situ Static Light Scattering", *Chem. Mater.* **23**: 2130 (2011)
19. Parra, et al., "Reaction Pathway to the Synthesis of Anatase via the Chemical Modification of Titanium Isopropoxide with Acetic Acid", *Chem. Mater.* **20**: 143 (2008)
20. K.W. Chapman, et al., "Radioactive Iodine Capture in Silver-Containing Mordenites through Nanoscale Silver Iodide Formation", *J. Amer. Chem. Soc.*, **132**(26): 8897 (2010)
21. D.F. Sava, et al., "Capture of Volatile Iodine, a Gaseous Fission Product, by Zeolitic Imidazolate Framework-8", *J. Amer. Chem. Soc.*, ***133***(32), 12398 (2011)

22. K.W. Chapman, et al., “Trapping Guests Within a Nanoporous Metal-Organic Framework Through Pressure-Induced Amorphization”, *J. Amer. Chem. Soc.*, ***133***(46), 18583 (2011)
23. D.F. Sava, et al., “Iodine Confinement into Metal-Organic Frameworks (MOFs): Low Temperature Sintering Glasses to form Novel Glass Composite Material (GCM) Alternative Waste Forms”, *Ind. Eng. Chem. Res*, **51** (2), 614 (2012)
24. J. Liu, et al., “Metal-Organic Frameworks for Removal of Xe and Kr from Nuclear Fuel Reprocessing Plants”. *Langmuir*, **28**: 11584 (2012)
25. C.A. Fernandez, et al., “Switching Kr/Xe Selectivity with Temperature in a Metal-Organic Framework”, *J. Amer. Chem. Soc.*, **134**(22):9046-9049 (2012)

Distribution

1 Terry Todd
Idaho National Laboratory
2525 Fremont Ave.
Idaho Falls, ID 83415

1 James Bresee
U.S. Department of Energy
1000 Independence Ave. SW
Washington, DC 20585

1 John Vienna
Pacific Northwest National Laboratory
P.O. Box 999
Richland, WA 99352

5 MS 1415 Haiqing Liu, 1114
1 MS 1415 Tina Nenoff, 1114
1 MS 1415 Carlos Gutierrez, 1114
1 MS 1411 Nelson S. Bell, 1816
1 MS 1415 Dorina F. Sava, 1114
1 MS 0747 Ben Cipiti, 6223
1 MS 1136 Tom Lewis, 6221
1 MS 0779 Kevin McMahon, 6222
1 MS 0899 Technical Library, 9536 (electronic copy)


Sandia National Laboratories